Hindawi
Journal of Nanomaterials
Volume 2019, Article ID 9214186, 8 pages
https://doi.org/10.1155/2019/9214186

Research Article

Triggering WORM/SRAM Memory Conversion by Composite Oxadiazole in Polymer Resistive Switching Device

Enming Zhao, Xiaodan Liu, Guangyu Liu, and Bao Zhou

School of Engineering, Dali University, Dali 671003, China

Correspondence should be addressed to Xiaodan Liu; liuxiaodandali@163.com

Received 14 April 2019; Accepted 1 July 2019; Published 21 August 2019

Guest Editor: Laijun Liu

Electrical characterization indicates that the nonvolatile write once read many (WORM) times/volatile static random access memory (SRAM) conversion was triggered by the composite of the oxadiazole small molecule. FTO/PMMA/Ag device possesses nonvolatile WORM memory behavior, while the FTO/PMMA+oxadiazole/Ag device shows vastly different volatile SRAM feature. The FTO/PMMA/Ag and FTO/PMMA+oxadiazole/Ag memory devices both exhibit high ON/OFF ratio nearly 10^4. The additive oxadiazole small molecule in the polymethyl methacrylate was suggested to form an internal electrode and serve as a channel during the charge transfer process, which is easy to both the charge transfer and back charge transfer, as a consequence, the WORM/SRAM conversion upon oxadiazole small molecule complexation was triggered. The results observed in this work manifest the significance of oxadiazole small molecule to the memory effects and will arouse the research interest about small molecule composite applied in memory devices.

1. Introduction

Resistive random access memory (RRAM) devices has aroused the research scholar's widespread interest on the account of their fast operation speed, simple construction, low power dissipation, and compatibility with conventional CMOS technique [1–4]. RRAM devices are probably a promising solution to traditional memory technologies facing the physical limit. On account of their widespread applications in nonvolatile data memory [5], logic operation [6–8], neuromorphic circuits [9], and programmable analogue circuits [10]. For resistive switching effect, the device could be repeatedly converted between the OFF state and the ON state, once an appropriate voltage is applied. Up till now, resistive switching has been reported in a variety of materials, for instance, perovskites [11], binary oxides [12], organics [13–16], TiO_x [17], $MoSe_2$-doped ultralong Se microwires [18], Fe_2O_3 solid electrolyte [8], and chalcogenide [19]. In particular, resistive switching memory integrated with nanogenerators for self-powered device has been developed recently [20]. During the last several years, organic resistive switching memory device has attracted special attention, such as polyvinyl carbazole [21], epoxy methacrylate resin [22], and poly(vinyl alcohol) [23]. Taking these into account, organic memory shows excellent mechanical flexibility, high ductility, excellent bendability, low cost, and the possibility for molecular design through chemical synthesis [24]. The charge transfer mechanisms in RRAM memory devices could be ascribed to various physical and/or chemical behavior theory and still needs more work [25].

In a variety of organic materials that were applied in the resistive switching memory devices, polymer has drawn a lot of attention on account of easy processing, favourable environmental stability, easiness in the fabrication of thin films, and low cost [26]. The application of the polymer made the flexible RRAM film devices possible. Flexible devices promise a broad application prospect [27, 28]. Integrating polymer with small molecule material has been recently investigated with the purpose of realizing preferable synergetic effects with the two materials [29].

Polymethyl methacrylate (PMMA) has been verified a polymeric matrix in resistive switching application [30, 31], which being a low cost and easily processed organic material, has more and more interest in flexible resistive switching

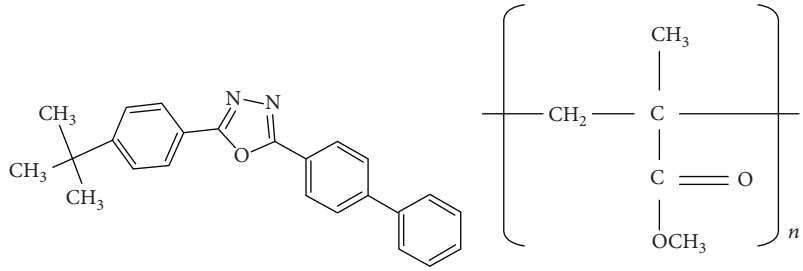

Figure 1: Chemical structure of oxadiazole and PMMA.

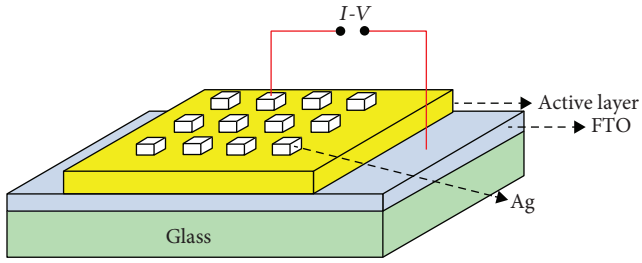

Figure 2: The structure of the memory device.

devices owing to its favourable switching and for its function as a normative resistance material in submicron RRAM lithography [32]. Simultaneously, oxadiazole derivatives were intensively reported as ideal electron acceptor materials in electronic devices [33–39]; 2-(4-tert-butylphenyl)-5-(4-biphenylyl)-1,3,4-oxadiazole was one of the most efficient electron-transporting materials on account of its high electron affinity. In the present work, PMMA is used as the host body for forming a thin film. And it was used to form the nanocomposite with 2-(4-tert-butylphenyl)-5-(4-biphenylyl)-1,3,4-oxadiazole to demonstrate resistive switching characteristics. And 2-(4-tert-butylphenyl)-5-(4-biphenylyl)-1,3,4-oxadiazole functions as the donor.

2. Experimental

The 2-(4-tert-butylphenyl)-5-(4-biphenylyl)-1,3,4-oxadiazole ($M_w = 354$, MDL: MFCD00003101) and PMMA (average $M_w = 150{,}000$, MDL: MFCD00134349) were both purchased from Sigma-Aldrich. The chemical structures of oxadiazole and PMMA are shown in Figure 1. To prepare PMMA+oxadiazole nanocomposites, 1 g of 2-(4-tert-butylphenyl)-5-(4-biphenylyl)-1,3,4-oxadiazole powder was mixed to 20 g of PMMA, then 5 g of the prepared composite was added to 50 ml of chlorobenzene solvent and PMMA in chlorobenzene solvent of 10 mg/ml with subsequent magnetic stirring for 48 h. After that, the PMMA+oxadiazole composite solution (filtered by polytetrafluoroethylene membrane, pore size of 0.22 mm) and PMMA of chlorobenzene solvent were spin-coated on a cleaned SnO_2 doped with fluorine (FTO) glass (purchased from Guluo Co. Ltd. Luoyang, China) at 800 rpm for 15 s, and then 4000 rpm for 60 s. Afterwards, the spin-coated FTO glasses were baked in 40°C for overnight on a hot plate to remove the residual solvent. The top Ag electrode with a thickness of 200 nm was deposited by using thermal evaporation under the pressure of 1×10^{-4} Pa. The fabricated structure of the memory device is schematically exhibited in Figure 2. The morphology of the cross-section properties of the active layer was tested by scanning electron microscopy (SEM; Nova Nano 450). All electrical measurements were performed by using a semiconductor characterization system (Keithley 4200) at room temperature. The bottom FTO electrode was grounded in the process of the resistive switching performance test, and an external voltage was applied to the top Ag electrode.

3. Results and Discussion

The cross-section SEM images of the PMMA and PMMA +oxadiazole composite films before the deposition of the top Ag electrode are shown in Figure 3.

The electrical memory behavior of the two devices was characterized by the current-voltage ($I - V$) curves of the FTO/PMMA/Ag and FTO/PMMA+oxadiazole/Ag sandwich devices. Figure 4(a) shows the $I - V$ curves of the FTO/PMMA/Ag memory device, which indicates a typical nonvolatile WORM performance. As seen in Figure 4(a), the FTO/PMMA/Ag device is initially in the high resistance state (the OFF state). In the process of the first positive voltage sweep, a sudden increase in current happened at the voltage of about 1.25 V, indicating the transition of the FTO/PMMA/Ag device from the high-resistance state to the low-resistance state (ON state) with an ON/OFF ratio up to 10^4 as shown in Figure 4(b). On this transformation, the FTO/PMMA/Ag device retains this ON state in the process of the succeeding positive scan (2nd sweep) and negative scan (3rd sweep) and cannot retrieve to its initial high-resistance state even though power supply shut down (4th sweep), manifesting its nonreversible nonvolatile nature and write once read many (WORM) times memory properties. Broadly speaking, the quantitative evaluation of resistive switching was assessed with the I_{OFF}/I_{ON} ratio at each applied voltage. This would help in providing information about the optimum operation parameters of the threshold resistive switching voltage (V_{th}) and the range of applied voltage for observing the obvious ON and OFF, and the amount of distinctiveness (I_{OFF}/I_{ON}) can result in defining the critical process parameters for the preparation of memory device structures with an efficient bipolar resistive switching behavior. Figure 4(b) describes the evaluated values for I_{OFF}/I_{ON} depending on the applied bias of the representative FTO/PMMA/Ag device structures. In order to assess the stability and reliability of the

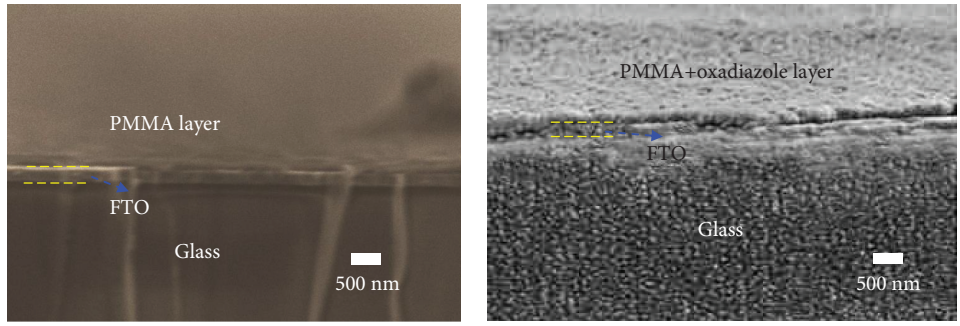

(a) (b)

Figure 3: (a) SEM images of PMMA layer films. (b) SEM images of PMMA+oxadiazole composite films.

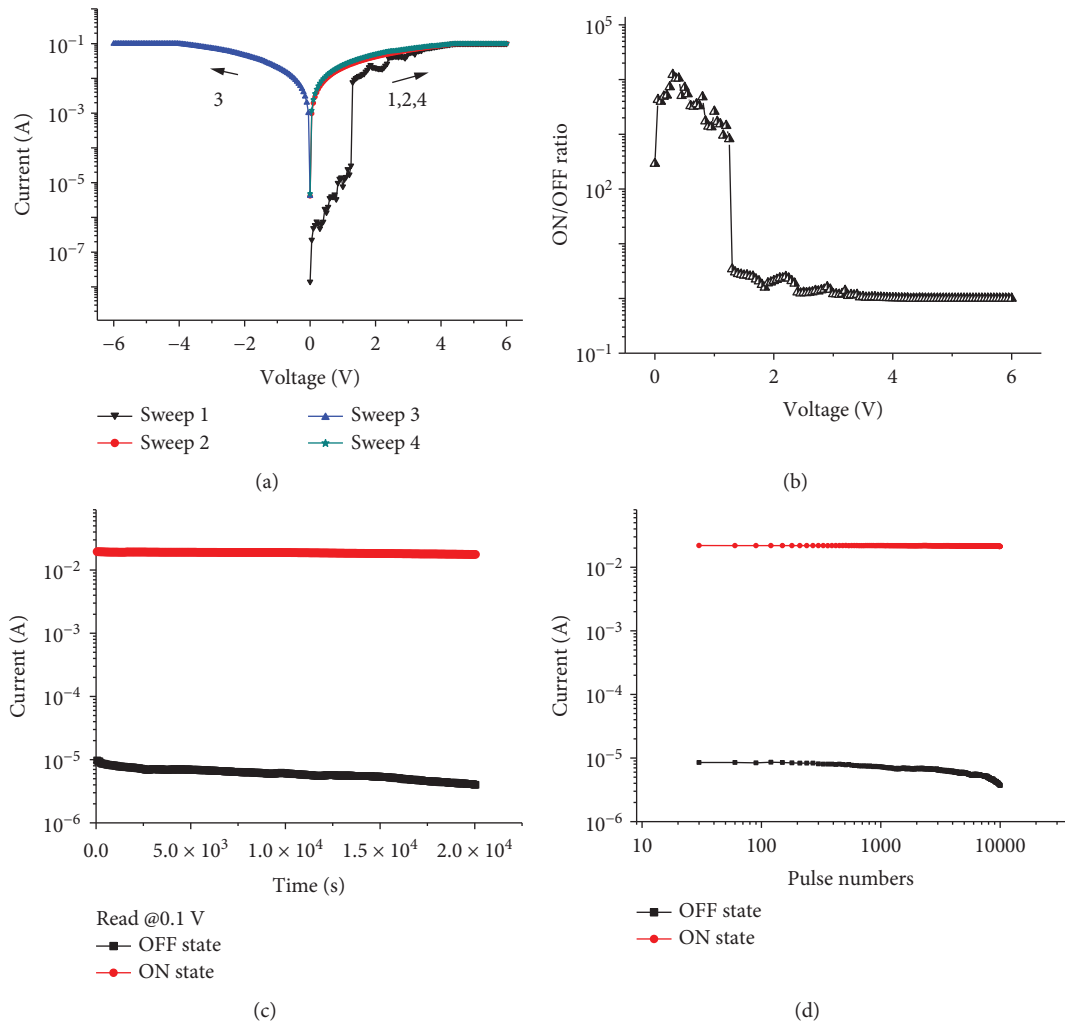

Figure 4: (a) $I - V$ curves of the FTO/PMMA/Ag device. (b) Switching ratio (I_{ON}/I_{OFF}) versus the applied bias, as estimated from the $I - V$ sweeps recorded for FTO/PMMA/Ag device. (c) Retention performance of the ON and OFF states of the FTO/PMMA/Ag device tested at 0.1 V. (d) Stimulus effect of 0.1 V read pulse under the ON and OFF states of the FTO/PMMA/Ag device.

FTO/PMMA/Ag memory behavior, Figures 4(c) and 4(d) show the performance of retention time and stimulus read pulse under the ON and OFF states of the FTO/PMMA/Ag device. Both ON and OFF states were tested under constant voltage stress and continuous pulse. No significant attenuation in current was observed, and both the ON and OFF current responses were fairly stable which reached up to 2×10^4 s and 10^4 continuous read pulses, manifesting favourable stability and reliability of the FTO/PMMA/Ag device.

Figure 5(a) shows the $I - V$ curves of the FTO/PMMA +oxadiazole/Ag device. Totally different from the FTO/PMMA/Ag memory device, the added 2-(4-tert-butylphenyl)-

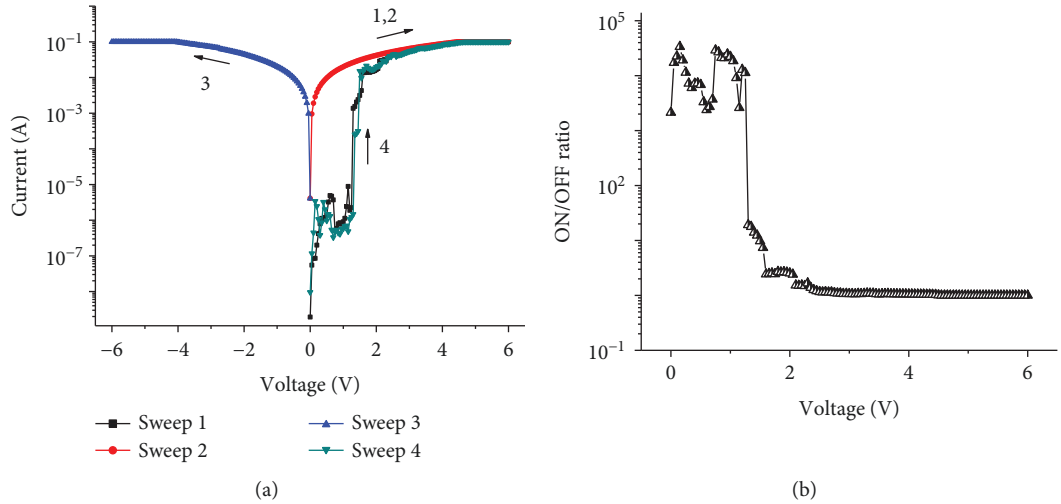

FIGURE 5: (a) $I - V$ curves of FTO/PMMA+oxadiazole/Ag device. (b) Switching ratio (I_{ON}/I_{OFF}) depends on the applied bias, as estimated from the $I - V$ sweeps recorded for FTO/PMMA+oxadiazole/Ag device.

5-(4-biphenylyl)-1,3,4-oxadiazole small molecule indicates a reversible volatile SRAM memory property, manifesting the important role of oxadiazole small molecule in the PMMA composite. As shown in Figure 5(a), in the process of the first positive sweep from 0 to 6 V, the FTO/PMMA+oxadiazole/Ag device maintains its OFF state until a threshold switching voltage of 1.30 V was reached. The current of the FTO/PMMA/Ag device then increased suddenly from 10^{-6} A to 10^{-2} A, converting the FTO/PMMA+oxadiazole/Ag device to the ON state. The FTO/PMMA+oxadiazole/Ag device stablely maintained in the ON state in the process of the continued positive and negative scan (2nd and 3rd sweeps). Nevertheless, the subsequent tests exhibit that the ON state can only be maintained transiently and will relax to the original OFF state spontaneously once cutting off power supply for over 3 min, manifesting its actually "volatile" feature. Then, in the fourth scan, the FTO/PMMA+oxadiazole/Ag device can be converted to the ON state again, manifesting its volatile static random access memory (SRAM) properties. The $I - V$ curves in Figure 5(a) indicate that the FTO/PMMA+oxadiazole/Ag takes on the volatile but reprogrammable electrical bistability, which could be applied in SRAM devices in digital information technology. Figure 5(b) shows the estimated values for comparable I_{OFF}/I_{ON} versus the applied voltage of representative FTO/PMMA+oxadiazole/Ag device structures. To this point, it could be confirmed that it must be the added-(4-tert-butylphenyl)-5-(4-biphenylyl)-1,3,4-oxadiazole small molecule which plays a vital function and has a significant change in the resistive switching process. The function of the oxadiazole small molecule is regarded as it serves as a medium or a charge transport channel, which affords a more convenient path for carrier transport and consequently be convenient for the electron-accepting process.

Comparative analyses of both devices' switching uniformity have been made between FTO/PMMA+oxadiazole/Ag and FTO/PMMA/Ag memory device. The cumulative distributions of resistive switching voltage (V_{th}) and resistance of ON and OFF states (R_{ON} and R_{OFF}) for FTO/PMMA+oxadiazole/Ag and FTO/PMMA/Ag device are shown in Figures 6(a)–6(d). For the sake of comparison and evaluation, the variation coefficients of all switching parameters have been calculated by σ/μ (where σ is the standard deviation and μ is the average value). Figure 6(e) shows the variation coefficients of V_{th}, R_{OFF}, and R_{ON}, respectively.

Figure 7 shows the UV-vis absorption spectra of the PMMA and the composite film of PMMA and oxadiazole small molecule. The PMMA and PMMA+oxadiazole show a distinct absorption peaks near 345.5 nm, respectively, both of which are corresponding to the $\pi - \pi*$ transition of PMMA. Obviously, the $\pi - \pi*$ absorption of the oxadiazole small molecule is blue-shifted, manifesting that the addition of oxadiazole in the PMMA matrix was beneficial to the $\pi - \pi*$ electron transitions of the PMMA, for which one considered reason is the ameliorated molecular coplanarity of the methacrylate methacrylic ring after oxadiazole small molecule composite. Whereas a weak absorption peak appeared at 301.5 nm, the absorption transitions were wholly blue-shifted to a lower wavelength region, manifesting the possible formation of oxadiazole chains aggregation, which will facilitate charge transfer in the PMMA bulk when the external bias was applied.

To better catch on the resistive switching mechanism, the $I - V$ characteristics were redrawn in the double-log coordinate system as exhibited in Figure 8. The ON state of the FTO/PMMA/Ag and FTO/PMMA+oxadiazole/Ag devices shows linearity in the $I - V$ relationship and the slope of the plot is nearly 1 (1.04 and 1.02), manifesting that the ohmic conduction through the conducting filament is dominant. In the OFF state of the FTO/PMMA/Ag and FTO/PMMA+oxadiazole/Ag device, the ohmic conduction was observed in a low voltage region, and the slope increased to over 2 (2.94, 1.19, and 3.78), manifesting that the space-charge-limited conduction (SCLC) among the disconnected portion of the conducting filament governs in a high voltage region. These conduction properties in

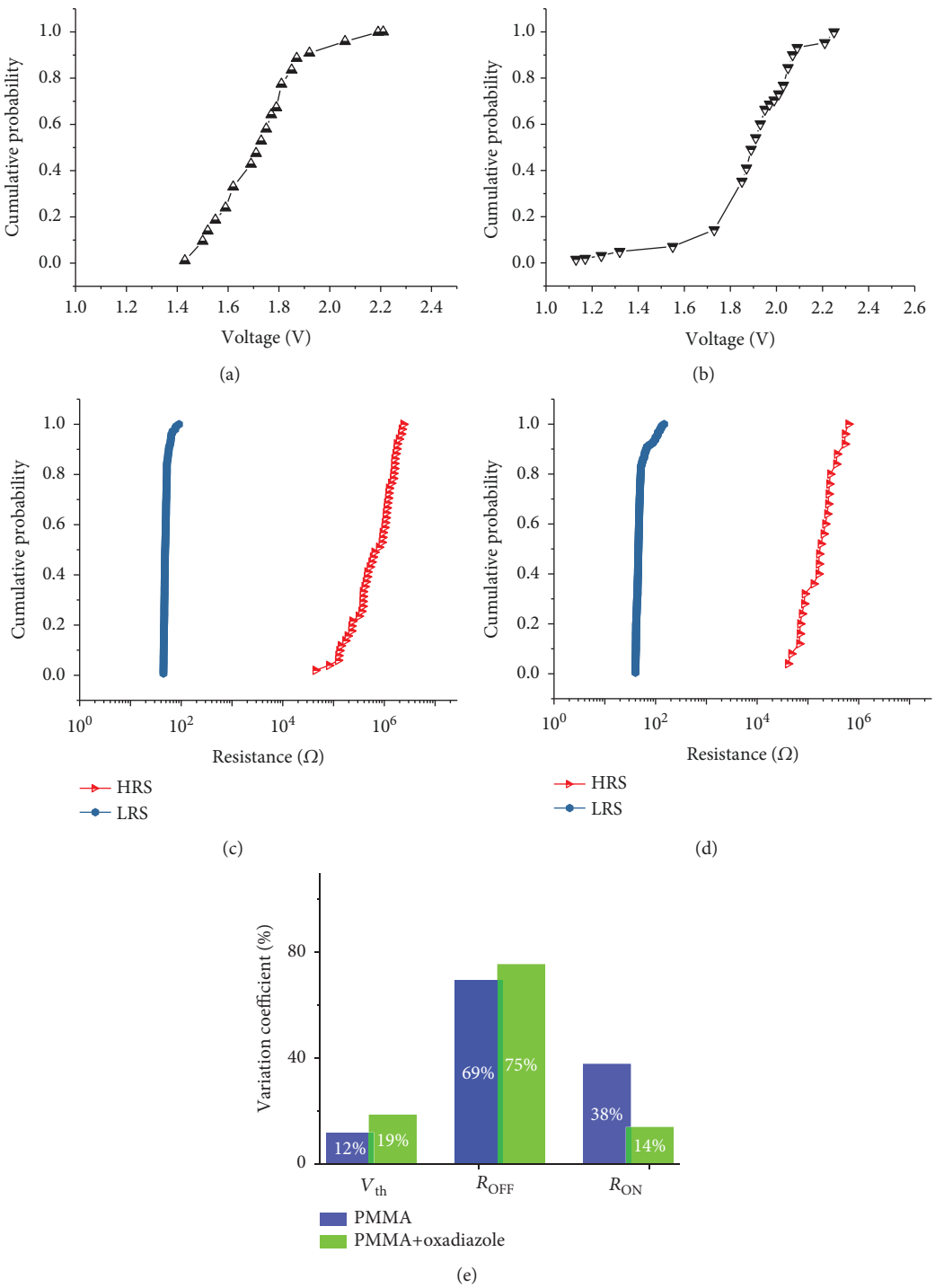

Figure 6: (a) Cumulative distributions of V_{th} for FTO/PMMA/Ag. (b) Cumulative distributions of V_{th} for FTO/PMMA+oxadiazole/Ag device. (c) Cumulative probability of R_{ON} and R_{OFF} for FTO/PMMA/Ag. (d) Cumulative probability of R_{ON} and R_{OFF} for FTO/PMMA +oxadiazole/Ag device. (e) Variation coefficients of V_{th}, R_{OFF}, and R_{ON}.

ON and OFF states are also in keeping with those in the previous report [40–42].

The experimental results indicate that the resistive switching property have a high association of the oxadiazole small molecule additives in polymer host. At initial stage, the charge carriers have no sufficient energy to overcome the charge injection barrier between PMMA molecules; the built-in electric field between the interface was formed [43–45], at the same time, the formation of built-in electric field will further hinder the injection of carriers. Thus, the FTO/PMMA/Ag device is on the high resistance state. Once the voltage scanning is up to the V_{th}, the occurrence of intermolecular charge transfer leads to transition in the FTO/PMMA/Ag device from OFF to ON state. The formed

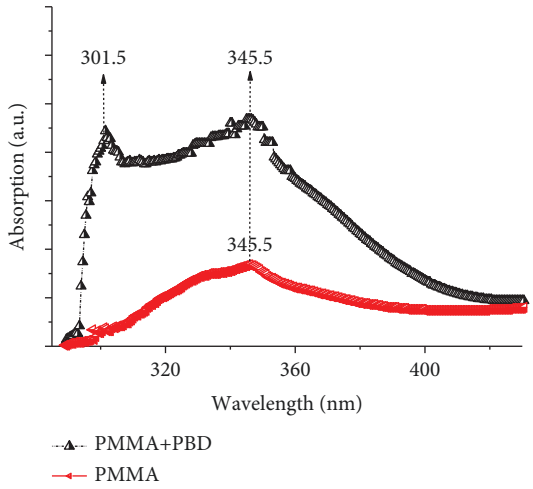

Figure 7: Absorption spectra of PMMA and PMMA+oxadiazole composite thin films.

charge transfer was in favour of the holding of the generated charge carriers, which may be related to the nonvolatility of the resulting data-storage devices. As indicated above, oxadiazole small molecule complexation has facilitated electron accepting in active layer and endows the active layer with a quasireversible *n*-doping feature, suggesting that the oxadiazole moieties in PMMA could act as mediators to facilitate the intramolecular charge transfer. Here, the quasireversible features of the oxadiazole group are supposed to be partially responsible for the reversible volatile SRAM memory behaviors for the FTO/PMMA+oxadiazole/Ag device. Because of the quasireversible and unstable charge transfer, the charge transfer state immediately dissociates via the back charge transfer or a recombination process of the separated charges after taking out the external power supply, which leads to volatile memory characteristic in FTO/PMMA+oxadiazole/Ag device.

4. Conclusions

In summary, small molecule oxadiazole was composited with polymer PMMA, which easily formed a thin film in this work for memory applications, that effectively avoids the defect of crystallization of small molecules during the formation of thin film. The FTO/PMMA/Ag device show irreversible nonvolatile WORM feature. However, after oxadiazole was added, the FTO/PMMA+oxadiazole/Ag device exhibits reversible volatile SRAM memory properties. More importantly, the added oxadiazole forms an internal electrode and serves as a medium in the process of charge transfer, which facilitates the forth and back charge transfers, furthermore triggering the conversion from WORM to SRAM memory. This work indicates the feasibility of oxadiazole in electronic resistive switching memory and demonstrates the consequence of oxadiazole complexation in the resistive switching memory effects, which would probably attract the interest of academic researchers to prepare desirable memory device by

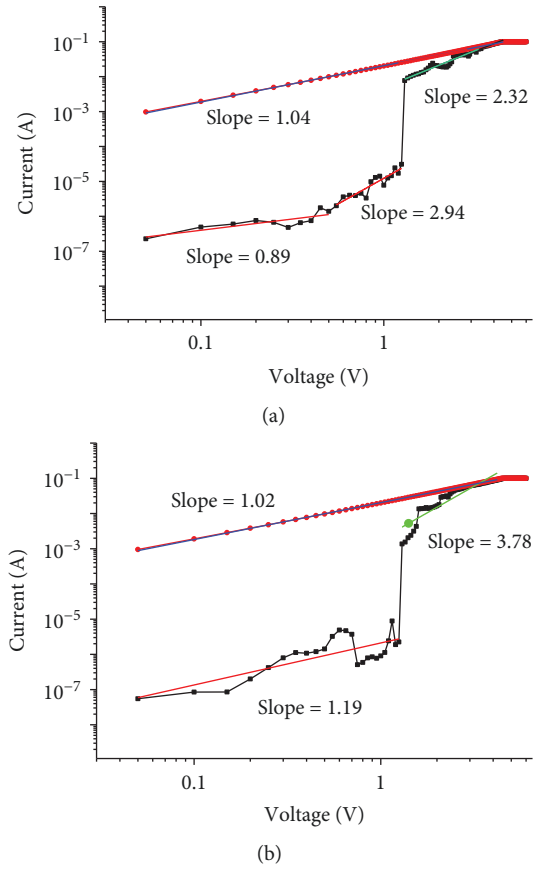

Figure 8: Double logarithm plot of $I - V$ curves.

using small molecule oxadiazole species and the memory effect of WORM to SRAM conversion application.

Data Availability

The data used to support the findings of this study are included within the article.

Conflicts of Interest

The authors declare that they have no conflicts of interest.

Acknowledgments

The authors acknowledge the financial support of the basic research project of the basic research business of the provincial higher school in Heilongjiang Province (RCCX201702).

References

[1] R. Waser, R. Dittmann, G. Staikov, and K. Szot, "Redox-based resistive switching memories—nanoionic mechanisms, prospects, and challenges," *Advanced Materials*, vol. 21, no. 25-26, pp. 2632–2663, 2009.

[2] G. Zhou, Z. Ren, L. Wang, B. Sun, S. Duan, and Q. Song, "Artificial and wearable albumen protein memristor arrays with integrated memory logic gate functionality," *Materials Horizons*, 2019.

[3] W. J. Liu, L. Chen, P. Zhou et al., "Chemical-vapor-deposited graphene as charge storage layer in flash memory device," *Journal of Nanomaterials*, vol. 2016, Article ID 6751497, 6 pages, 2016.

[4] J. R. Rani, S. I. Oh, J. M. Woo, and J. H. Jang, "Low voltage resistive memory devices based on graphene oxide-iron oxide hybrid," *Carbon*, vol. 94, pp. 362–368, 2015.

[5] B. Sun, Y. X. Liu, L. F. Liu et al., "Highly uniform resistive switching characteristics of TiN/ZrO_2/ Pt memory devices," *Journal of Applied Physics*, vol. 105, no. 6, p. 061630, 2009.

[6] E. Linn, R. Rosezin, S. Tappertzhofen, U. Böttger, and R. Waser, "Beyond von Neumann-logic operations in passive crossbar arrays alongside memory operations," *Nanotechnology*, vol. 23, no. 30, p. 305205, 2012.

[7] M. S. Kadhim, F. Yang, B. Sun et al., "Existence of resistive switching memory and negative differential resistance state in self-colored MoS_2/ZnO heterojunction devices," *ACS Applied Electronic Materials*, vol. 1, no. 3, pp. 318–324, 2019.

[8] G. Zhou, X. Yang, L. Xiao, B. Sun, and A. Zhou, "Investigation of a submerging redox behavior in Fe2O3solid electrolyte for resistive switching memory," *Applied Physics Letters*, vol. 114, no. 16, p. 163506, 2019.

[9] T. Shi, X. B. Yin, R. Yang, and X. Guo, "Pt/WO_3/FTO memristive devices with recoverable pseudo-electroforming for time-delay switches in neuromorphic computing," *Physical Chemistry Chemical Physics*, vol. 18, no. 14, pp. 9338–9343, 2016.

[10] J. Zha, H. Huang, and Y. Liu, "A novel window function for memristor model with application in programming analog circuits," *IEEE Transactions on Circuits and Systems*, vol. 63, no. 5, pp. 423–427, 2016.

[11] F. Lv, C. Gao, H.-A. Zhou, P. Zhang, K. Mi, and X. Liu, "Nonvolatile bipolar resistive switching behavior in the perovskite-like $(CH_3NH_3)_2FeCl_4$," *ACS Applied Materials & Interfaces*, vol. 8, no. 29, pp. 18985–18990, 2016.

[12] B. Singh and B. R. Mehta, "Relationship between nature of metal-oxide contacts and resistive switching properties of copper oxide thin film based devices," *Thin Solid Films*, vol. 569, pp. 35–43, 2014.

[13] B. Cho, S. Song, Y. Ji, T.-W. Kim, and T. Lee, "Organic resistive memory devices: performance enhancement, integration, and advanced architectures," *Advanced Functional Materials*, vol. 21, no. 15, pp. 2806–2829, 2011.

[14] B. Sun, X. Zhang, G. Zhou et al., "An organic nonvolatile resistive switching memory device fabricated with natural pectin from fruit peel," *Organic Electronics*, vol. 42, pp. 181–186, 2017.

[15] B. Sun, S. Zhu, S. Mao et al., "From dead leaves to sustainable organic resistive switching memory," *Journal of Colloid and Interface Science*, vol. 513, pp. 774–778, 2018.

[16] Y. Sun, J. Lu, C. Ai, D. Wen, and X. Bai, "Enhancement of memory margins in the polymer composite of [6,6]-phenyl-C61-butyric acid methyl ester and polystyrene," *Physical Chemistry Chemical Physics*, vol. 18, no. 44, pp. 30808–30814, 2016.

[17] G. Zhou, S. Duan, P. Li et al., "Coexistence of negative differential resistance and resistive switching memory at room temperature in TiO_x modulated by moisture," *Advanced Electronic Materials*, vol. 4, no. 4, p. 1700567, 2018.

[18] G. Zhou, B. Sun, Y. Yao et al., "Investigation of the behaviour of electronic resistive switching memory based on $MoSe_2$-doped ultralong Se microwires," *Applied Physics Letters*, vol. 109, no. 14, p. 143904, 2016.

[19] A. Pradel, N. Frolet, M. Ramonda, A. Piarristeguy, and M. Ribes, "Bipolar resistance switching in chalcogenide materials," *Physica Status Solidi*, vol. 208, no. 10, pp. 2303–2308, 2011.

[20] G. Zhou, Z. Ren, L. Wang et al., "Resistive switching memory integrated with amorphous carbon-based nanogenerators for self-powered device," *Nano Energy*, vol. 63, p. 103793, 2019.

[21] Y. Sun, D. Wen, and F. Sun, "Influence of blending ratio on resistive switching effect in donor-acceptor type composite of PCBM and PVK-based memory devices," *Organic Electronics*, vol. 65, pp. 141–149, 2019.

[22] Y. Sun, J. Lu, C. Ai, D. Wen, and X. Bai, "Multilevel resistive switching and nonvolatile memory effects in epoxy methacrylate resin and carbon nanotube composite films," *Organic Electronics*, vol. 32, pp. 7–14, 2016.

[23] Y. Sun, J. Lu, C. Ai, and D. Wen, "Nonvolatile memory devices based on poly(vinyl alcohol)+graphene oxide hybrid composites," *Physical Chemistry Chemical Physics*, vol. 18, no. 16, pp. 11341–11347, 2016.

[24] Y. Sun, F. Miao, and R. Li, "Bistable electrical switching and nonvolatile memory effect based on the thin films of polyurethane-carbon nanotubes blends," *Sensors and Actuators A: Physical*, vol. 234, pp. 282–289, 2015.

[25] D. Chaudhary, S. Munjal, N. Khare, and V. D. Vankar, "Bipolar resistive switching and nonvolatile memory effect in poly (3-hexylthiophene)-carbon nanotube composite films," *Carbon*, vol. 130, pp. 553–558, 2018.

[26] Y. Li and X. Ni, "One-step preparation of graphene oxide–poly(3,4-ethylenedioxythiophene) composite films for nonvolatile rewritable memory devices," *RSC Advances*, vol. 6, no. 20, pp. 16340–16347, 2016.

[27] G. Khurana, P. Misra, and R. S. Katiyar, "Multilevel resistive memory switching in graphene sandwiched organic polymer heterostructure," *Carbon*, vol. 76, pp. 341–347, 2014.

[28] Y. Chen, G. Liu, C. Wang, W. Zhang, R.-W. Li, and L. Wang, "Polymer memristor for information storage and neuromorphic applications," *Materials Horizons*, vol. 1, no. 5, pp. 489–506, 2014.

[29] S. Miao, Y. Zhu, Q. Bao et al., "Solution-processed small molecule donor/acceptor blends for electrical memory devices with fine-tunable storage performance," *Journal of Physical Chemistry C*, vol. 118, no. 4, pp. 2154–2160, 2014.

[30] H. Y. Tsao, Y. W. Wang, and Z. K. Gao, "Resistive switching behavior of Ag/PMMA:Na/Ag devices for memory applications," *Thin Solid Films*, vol. 612, pp. 61–65, 2016.

[31] B. Cheng, J. Zhao, L. Xiao et al., "PMMA interlayer-modulated memory effects by space charge polarization in resistive switching based on CuSCN-nanopyramids/ZnO-nanorods p-n heterojunction," *Scientific Reports*, vol. 5, no. 1, 2015.

[32] J.-W. Lee and W.-J. Cho, "Fabrication of resistive switching memory based on solution processed PMMA-HfO_x blended thin films," *Semiconductor Science and Technology*, vol. 32, no. 2, p. 025009, 2017.

[33] Y. Sun, L. Li, D. Wen, and X. Bai, "Bistable electrical switching characteristics and memory effect by mixing of oxadiazole in polyurethane layer," *Journal of Physical Chemistry C*, vol. 119, no. 33, pp. 19520–19525, 2015.

[34] L. Pan, B. Hu, X. Zhu et al., "Role of oxadiazole moiety in different D-A polyazothines and related resistive switching

properties," *Journal of Materials Chemistry C*, vol. 1, no. 30, pp. 4556–4564, 2013.

[35] C. Weng, Z. Liu, H. Guo, and S. Tan, "The photoelectric properties of polymer acceptors containing oxadiazole and thiadiazole," *Macromolecular Chemistry and Physics*, vol. 218, no. 16, 2017.

[36] Y. Sun, L. Li, D. Wen, and X. bai, "Bistable electrical switching and nonvolatile memory effect in mixed composite of oxadiazole acceptor and carbazole donor," *Organic Electronics*, vol. 25, pp. 283–288, 2015.

[37] Y. Sun, F. Miao, R. Li, and D. Wen, "Resistive switching memory devices based on electrical conductance tuning in poly(4-vinyl phenol)-oxadiazole composites," *Physical Chemistry Chemical Physics*, vol. 17, no. 44, pp. 29978–29984, 2015.

[38] S. Levent, B. Kaya Çavuşoğlu, B. Sağlık et al., "Synthesis of oxadiazole-thiadiazole hybrids and their anticandidal activity," *Molecules*, vol. 22, no. 11, p. 2004, 2017.

[39] K. Kim, Y. K. Fang, W. Kwon, S. Pyo, W. C. Chen, and M. Ree, "Tunable electrical memory characteristics of brush copolymers bearing electron donor and acceptor moieties," *Journal of Materials Chemistry C*, vol. 1, no. 32, pp. 4858–4868, 2013.

[40] Y. Sun, D. Wen, and X. Bai, "Nonvolatile ternary resistive switching memory devices based on the polymer composites containing zinc oxide nanoparticles," *Physical Chemistry Chemical Physics*, vol. 20, no. 8, pp. 5771–5779, 2018.

[41] G. S. Kim, T. H. Park, H. J. Kim et al., "Investigation of the retention performance of an ultra-thin HfO_2 resistance switching layer in an integrated memory device," *Journal of Applied Physics*, vol. 124, no. 2, p. 024102, 2018.

[42] Y. Sun, D. Wen, X. Bai, J. Lu, and C. Ai, "Ternary resistance switching memory behavior based on graphene oxide embedded in a polystyrene polymer layer," *Scientific Reports*, vol. 7, no. 1, p. 3938, 2017.

[43] P. Zheng, B. Sun, Y. Chen et al., "Photo-induced negative differential resistance in a resistive switching memory device based on $BiFeO_3$/ZnO heterojunctions," *Applied Materials Today*, vol. 14, pp. 21–28, 2019.

[44] Y. Sun and D. Wen, "Conductance quantization in nonvolatile resistive switching memory based on the polymer composite of zinc oxide nanoparticles," *Journal of Physical Chemistry C*, vol. 122, no. 19, pp. 10582–10591, 2018.

[45] B. Sun, W. Zhao, Y. Liu, and P. Chen, "Resistive switching effect of Ag/MoS_2/FTO device," *Functional Materials Letters*, vol. 08, no. 01, p. 1550010, 2015.